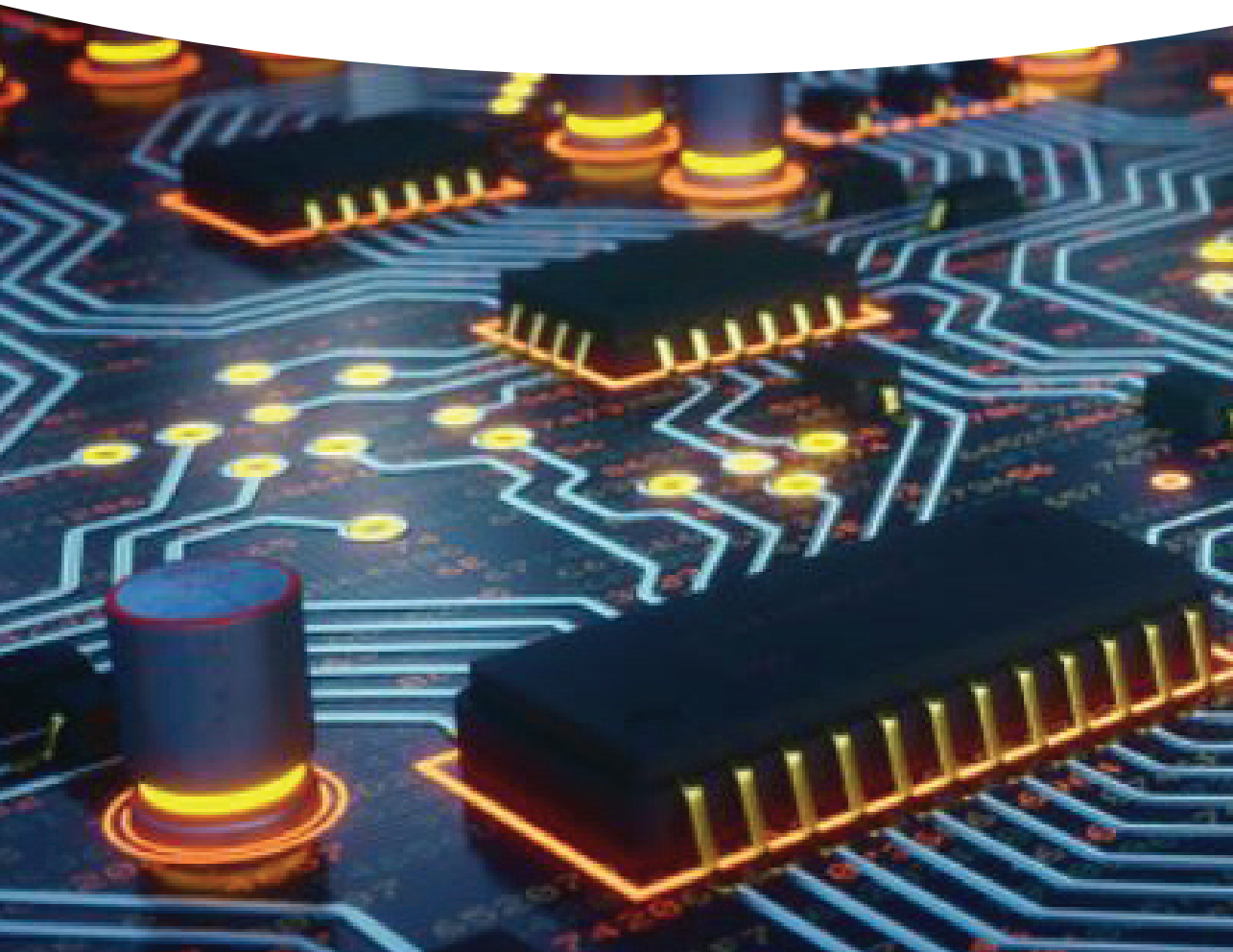


Teuvo Suntio, Tuomas Messo,
and Joonas Puukko

Power Electronic Converters

Dynamics and Control in Conventional
and Renewable Energy Applications



Teuvo Suntio

Tuomas Messo

Joonas Puukko

Power Electronic Converters

Power Electronic Converters

Dynamics and Control in Conventional and
Renewable Energy Applications

Teuvo Suntio, Tuomas Messo, and Joonas Puukko

Authors

Dr. Teuvo Suntio

Tampere University of Technology
Laboratory of Electrical Energy Engineering
Korkeakoulunkatu 3
33101 Tampere
Finland

Assist. Prof. Dr. Tuomas Messo

Tampere University of Technology
Laboratory of Electrical Energy Engineering
Korkeakoulunkatu 3
33101 Tampere
Finland

Dr. Joonas Puukko

ABB Oy
Drives
Hiomotie 13
00380 Helsinki
Finland

Cover

iStock ID 536657616/matejmo

■ All books published by **Wiley-VCH** are carefully produced. Nevertheless, authors, editors, and publisher do not warrant the information contained in these books, including this book, to be free of errors. Readers are advised to keep in mind that statements, data, illustrations, procedural details or other items may inadvertently be inaccurate.

Library of Congress Card No.: applied for

British Library Cataloguing-in-Publication Data

A catalogue record for this book is available from the British Library.

Bibliographic information published by the Deutsche Nationalbibliothek

The Deutsche Nationalbibliothek lists this publication in the Deutsche Nationalbibliografie; detailed bibliographic data are available on the Internet at <<http://dnb.d-nb.de>>.

© 2018 Wiley-VCH Verlag GmbH & Co. KGaA, Boschstr. 12, 69469 Weinheim, Germany

All rights reserved (including those of translation into other languages). No part of this book may be reproduced in any form – by photoprinting, microfilm, or any other means – nor transmitted or translated into a machine language without written permission from the publishers. Registered names, trademarks, etc. used in this book, even when not specifically marked as such, are not to be considered unprotected by law.

Print ISBN: 978-3-527-34022-4

ePDF ISBN: 978-3-527-69851-6

ePub ISBN: 978-3-527-69853-0

Mobi ISBN: 978-3-527-69854-7

oBook ISBN: 978-3-527-69852-3

Cover Design Wiley

Typesetting Thomson Digital, Noida, India

Printing and Binding Weinheim

Printed on acid-free paper

Table of Contents

Preface *xiii*

About the Authors *xv*

Part One Introduction *1*

1 Introduction *3*

1.1 Introduction *3*

1.2 Implementation of Current-Fed Converters *6*

1.3 Dynamic Modeling of Power Electronic Converters *7*

1.4 Linear Equivalent Circuits *8*

1.5 Impedance-Based Stability Assessment *12*

1.6 Time Domain-Based Dynamic Analysis *14*

1.7 Renewable Energy System Principles *17*

1.8 Content Review *19*

References *20*

2 Dynamic Analysis and Control Design Preliminaries *27*

2.1 Introduction *27*

2.2 Generalized Dynamic Representations – DC–DC *27*

2.2.1 Introduction *27*

2.2.2 Generalized Dynamic Representations *29*

2.2.3 Generalized Closed-Loop Dynamics *30*

2.2.4 Generalized Cascaded Control Schemes *33*

2.2.5 Generalized Source and Load Interactions *38*

2.2.6 Generalized Impedance-Based Stability Assessment *40*

2.3 Generalized Dynamic Representations: DC–AC, AC–DC, and AC–AC *42*

2.3.1 Introduction *42*

2.3.2 Generalized Dynamic Representations *44*

2.3.3 Generalized Closed-Loop Dynamics *48*

2.3.4 Generalized Cascaded Control Schemes *50*

2.3.5 Generalized Source and Load Interactions *54*

2.3.6 Generalized Impedance-Based Stability Assessment *56*

2.4	Small-Signal Modeling	57
2.4.1	Introduction	57
2.4.2	Average Modeling and Linearization	60
2.4.3	Modeling Coupled-Inductor Converters	64
2.4.4	Modeling in Synchronous Reference Frame	66
2.5	Control Design Preliminaries	77
2.5.1	Introduction	77
2.5.2	Transfer Functions	77
2.5.3	Stability	84
2.5.4	Transient Performance	95
2.5.5	Feedback-Loop Design Constraints	100
2.5.6	Controller Implementations	103
2.5.7	Optocoupler Isolation	108
2.5.8	Application of Digital Control	109
2.6	Resonant LC-Type Circuits	110
2.6.1	Introduction	110
2.6.2	Single-Section LC Filter	112
2.6.3	LCL Filter	113
2.6.4	CLCL Filter	115
	References	117

Part Two Voltage-Fed DC–DC Converters 123

3	Dynamic Modeling of Direct-on-Time Control	125
3.1	Introduction	125
3.2	Direct-on-Time Control	127
3.3	Generalized Modeling Technique	129
3.3.1	Buck Converter	131
3.3.2	Boost Converter	134
3.3.3	Buck–Boost Converter	136
3.3.4	Superbuck Converter	140
3.4	Fixed-Frequency Operation in CCM	142
3.4.1	Buck Converter	143
3.4.2	Boost Converter	146
3.4.3	Buck–Boost Converter	149
3.4.4	Superbuck Converter	153
3.4.5	Coupled-Inductor Superbuck Converter	157
3.5	Fixed-Frequency Operation in DCM	163
3.5.1	Buck Converter	164
3.5.2	Boost Converter	167
3.5.3	Buck–Boost Converter	170
3.6	Source and Load Interactions	173
3.6.1	Source Interactions	173
3.6.2	Input Voltage Feedforward	174
3.6.3	Load Interactions	176
3.6.4	Output-Current Feedforward	177

3.7	Impedance-Based Stability Issues	179
3.8	Dynamic Review	181
	References	186
4	Dynamic Modeling of Current-Mode Control	189
4.1	Introduction	189
4.2	Peak Current Mode Control	190
4.2.1	PCM Control Principles	190
4.2.2	Development of Duty-Ratio Constraints in CCM	192
4.2.3	Development of Duty-Ratio Constraints in DCM	195
4.2.4	Origin and Consequences of Mode Limits in CCM and DCM	196
4.2.5	Duty-Ratio Constraints in CCM	201
4.2.5.1	Buck Converter	201
4.2.5.2	Boost Converter	201
4.2.5.3	Buck–Boost Converter	202
4.2.5.4	Superbuck Converter	204
4.2.5.5	Coupled-Inductor Superbuck Converter	205
4.2.6	Duty-Ratio Constraints in DCM	205
4.2.6.1	Buck Converter	205
4.2.6.2	Boost Converter	206
4.2.6.3	Buck–Boost Converter	206
4.2.7	General PCM Transfer Functions in CCM	207
4.2.8	PCM State Spaces and Transfer Functions in CCM	209
4.2.8.1	Buck Converter	209
4.2.8.2	Boost Converter	211
4.2.8.3	Buck–Boost Converter	213
4.2.8.4	Superbuck Converter	215
4.2.8.5	Coupled-Inductor Superbuck Converter	219
4.2.9	PCM State Spaces in DCM	222
4.2.9.1	Buck Converter	222
4.2.9.2	Boost Converter	222
4.2.9.3	Buck–Boost Converter	223
4.3	Average Current-Mode Control	224
4.3.1	Introduction	224
4.3.2	ACM Control Principle	225
4.3.3	Modeling with Full Ripple Inductor Current Feedback	226
4.4	Variable-Frequency Control	230
4.4.1	Introduction	230
4.4.2	Self-Oscillation Modeling – DOT and PCM Control	231
4.5	Source and Load Interactions	239
4.5.1	Output Current Feedforward	240
4.6	Impedance-Based Stability Issues	243
4.7	Dynamic Review	244
4.8	Critical Discussions on PCM Models and Their Validation	249
4.8.1	Ridley's Models	249
4.8.2	The Book PCM Model in CCM	252

4.8.3	Evaluation of PCM-Controlled Buck in CCM	253
4.8.4	Evaluation of PCM-Controlled Boost in CCM	258
4.8.5	Concluding Remarks	259
	References	260
5	Dynamic Modeling of Current-Output Converters	265
5.1	Introduction	265
5.2	Dynamic Modeling	267
5.3	Source and Load Interactions	269
5.3.1	Source Interactions	269
5.3.2	Load Interactions	270
5.4	Impedance-Based Stability Issues	271
5.5	Dynamic Review	272
	References	275
6	Control Design Issues in Voltage-Fed DC–DC Converters	277
6.1	Introduction	277
6.2	Developing Switching and Average Models	279
6.2.1	Switching Models	279
6.2.2	Averaged Models	287
6.3	Factors Affecting Transient Response	291
6.3.1	Output Voltage Undershoot	292
6.3.2	Settling Time	294
6.4	Remote Sensing	304
6.4.1	Introduction	304
6.4.2	Remote Sensing Dynamic Effect Analysis Method	304
6.4.3	Remote Sensing Impedance Block Examples	306
6.4.4	Experimental Evidence	307
6.5	Simple Control Design Method	310
6.5.1	DDR-Controlled Buck Converter	312
6.5.2	PCM-Controlled Buck Converter	315
6.5.3	DDR-Controlled Boost Converter	321
6.5.4	PCM-Controlled Boost Converter	325
6.6	PCM-Controlled Superbuck Converter: Experimental Examples	330
6.6.1	Introduction	330
6.6.2	Discrete-Inductor Superbuck	331
6.6.3	Coupled-Inductor Superbuck	332
6.7	Concluding Remarks	334
	References	334
Part Three	Current-Fed Converters	339
7	Introduction to Current-Fed Converters	341
7.1	Introduction	341
7.2	Duality Transformation Basics	341
7.3	Duality-Transformed Converters	345

7.4	Input Capacitor-Based Converters	351
	References	352
8	Dynamic Modeling of DDR-Controlled CF Converters	355
8.1	Introduction	355
8.2	Dynamic Models	356
8.2.1	Duality Transformed Converters	358
8.2.1.1	Buck Converter	358
8.2.1.2	Boost Converter	365
8.2.1.3	Noninverting Buck–Boost Converter	368
8.2.1.4	CF Superbuck Converter	372
8.2.2	Input Capacitor-Based Converters	376
8.2.2.1	Buck Power-Stage Converter	377
8.2.2.2	Boost Power-Stage Converter	383
8.2.2.3	Noninverting Buck–Boost Power-Stage Converter	387
8.3	Source and Load Interactions	390
8.3.1	CF-CO Converters	390
8.3.1.1	Source Interactions	390
8.3.1.2	Load Interactions	391
8.3.2	CF-VO Converters	392
8.3.2.1	Source Interactions	392
8.3.2.2	Load Interactions	393
8.4	Impedance-Based Stability Assessment	394
8.5	Output-Voltage Feedforward	394
8.6	Dynamic Review	397
	References	400
9	Dynamic Modeling of PCM/PVM-Controlled CF Converters	403
9.1	Introduction	403
9.2	Duty-Ratio Constraints and Dynamic Models under PCM Control	404
9.2.1	Buck Power-Stage Converter	405
9.2.2	Boost Power-Stage Converter	410
9.3	Duty-Ratio Constraints and Dynamic Models under PVM Control	413
9.3.1	CF Buck Converter	414
9.3.2	CF Superbuck Converter	418
9.4	Concluding Remarks	420
	References	420
10	Introduction to Photovoltaic Generator	423
10.1	Introduction	423
10.2	Solar Cell Properties	424
10.3	PV Generator	429
10.4	MPP Tracking Methods	432
10.5	MPP Tracking Design Issues	436
10.5.1	Introduction	436
10.5.2	General Dynamics of PV Power	437
10.5.3	PV Interfacing Converter Operating at Open Loop	439

10.5.4	PV Interfacing Converter Operating at Closed Loop	447
10.5.4.1	Reduced-Order Models: Intuitive Model Reduction	452
10.5.4.2	Reduced-Order Models: Control-Engineering-Based Method	454
10.5.4.3	Reduced-Order Model Verification	455
10.6	Concluding Remarks	461
	References	461
11	Photovoltaic Generator Interfacing Issues	465
11.1	Introduction	465
11.2	Centralized PV System Architecture	465
11.3	Distributed PV System Architectures	465
11.4	PV Generator-Induced Effects on Interfacing-Converter Dynamics	470
11.4.1	Introduction	470
11.4.2	PV Generator Effects on Converter Dynamics	474
11.4.2.1	Buck Power-Stage Converter	476
11.4.2.2	Boost Power-Stage Converter	477
11.4.2.3	CF Superbuck Converter	480
11.5	Stability Issues in PV Generator Interfacing	482
11.5.1	Buck Power-Stage Converter	483
11.5.2	CF Superbuck Converter	485
11.5.3	Concluding Remarks	488
11.6	Control Design Issues	488
	References	488
Part Four	Three-Phase Grid-Connected Converters	491
12	Dynamic Modeling of Three-Phase Inverters	493
12.1	Introduction	493
12.2	Dynamic Model of Voltage-Fed Inverter	494
12.2.1	Average Model of Voltage-Fed Inverter	494
12.2.2	Linearized State-Space and Open-Loop Dynamics	499
12.2.3	Control Block Diagrams of Voltage-Fed Inverter	503
12.2.4	Verification of Open-Loop Model	503
12.3	Dynamic Model of Current-Fed Inverter	507
12.3.1	Average Model of Current-Fed Inverter	507
12.3.2	Linearized Model and Open-Loop Dynamics	510
12.3.3	Control Block Diagrams of Current-Fed Inverter	512
12.3.4	Verification of Open-Loop Model	512
12.4	Source-Affected Dynamics of Current-Fed Inverter	515
12.4.1	Source Effect: Photovoltaic Generator	517
12.4.2	Source Effect: Experimental Validation	520
12.5	Dynamic Model of Current-Fed Inverter with LCL-Filter	524
12.5.1	Average Model of Current-Fed Inverter with LCL-Filter	525

12.5.2	Linearized State-Space and Open-Loop Dynamics	527
12.6	Summary	528
Appendix 12.A		528
References		530
13	Control Design of Grid-Connected Three-Phase Inverters	533
13.1	Introduction	533
13.2	Synchronous Reference Frame Phase-Locked-Loop	533
13.2.1	Linearized Model of SRF-PLL	536
13.2.2	Control Design of SRF-PLL	538
13.2.3	Damping Ratio and Undamped Natural Frequency	541
13.2.4	Control Design Example and Experimental Verification	541
13.2.5	The Effect of Unbalanced Grid Voltages	544
13.3	AC Current Control	547
13.3.1	Current Control in the dq-Domain	548
13.3.2	Current Control in Voltage-Fed Inverters	548
13.4	Decoupling Gains	559
13.5	Grid Voltage Feedforward	562
13.6	Cascaded Control Scheme in Current-Fed Inverters	563
13.6.1	Control Block Diagrams	564
13.6.2	Control Design of Cascaded Loops	566
13.6.3	Instability Caused by RHP-Pole	570
13.6.4	Stability Assessment Using the Nyquist Stability Criterion	574
13.6.5	Design Example: Three-Phase Photovoltaic Inverter	574
13.7	Case Study: Instability Due to RHP-Pole	581
13.8	Summary	583
References		583
14	Reduced-Order Closed-Loop Modeling of Inverters	587
14.1	Introduction	587
14.2	Reduced-Order Model of Voltage-Fed Inverter	587
14.2.1	Closed-Loop Model with AC Current Control	588
14.2.2	Closed-Loop Model with SRF-PLL	591
14.2.3	Closed-Loop Input Admittance	595
14.2.4	Output Impedance with Grid Voltage Feedforward	596
14.2.5	Impedance Characteristics of Voltage-Fed Inverters	602
14.3	Reduced-Order Model of Current-Fed Inverter with L-Type Filter	602
14.3.1	Closed-Loop Model with Cascaded Control Scheme	602
14.3.2	Effect of Input Voltage Control Bandwidth	605
14.3.3	Effect of AC Current Control Bandwidth	606
14.3.4	Experimental Verification: Measured Impedance d-Component	608
14.3.5	Effect of SRF-PLL	609
14.3.6	Effect of Grid Voltage Feedforward on Impedance d-Component	610
14.3.7	Effect of Grid Voltage Feedforward on Impedance q-Component	615

14.4	Closed-Loop Model of Current-Fed Inverter with LC-Type Filter	619
14.4.1	Experimental Verification of Impedance Model	625
14.4.2	Impedance Characteristics of Inverter with LC-Filter and Feedforward	630
14.5	Summary	630
	References	630
15	Multivariable Closed-Loop Modeling of Inverters	633
15.1	Introduction	633
15.2	Full-Order Model of Current-Fed Inverter with L-Type Filter	633
15.2.1	Verification of Dynamic Model	643
15.3	Experimental Verification of Admittance Model	646
15.4	Full-Order Model of Current-Fed Inverter with LCL-Type Filter	648
15.4.1	Verification of Closed-Loop Model	653
15.4.2	Measured Output Impedance of PV Inverter	656
15.5	Summary	659
	References	660
16	Impedance-Based Stability Assessment	663
16.1	Introduction	663
16.2	Modeling of Three-Phase Load Impedance in the dq -Domain	664
16.3	Impedance-Based Stability Criterion	667
16.4	Case Studies	669
16.4.1	Instability Due to High-Bandwidth PLL in Weak Grid	669
16.4.2	Instability Due to Control Delay in Feedforward Path	674
16.5	Summary	678
	References	678
17	Dynamic Modeling of Three-Phase Active Rectifiers	681
17.1	Introduction	681
17.2	Open-Loop Dynamics	681
17.3	Verification of Open-Loop Model	688
17.4	Experimental Results	691
17.5	Summary	695
	References	695
	Index	697

Preface

Rigid voltage sources, such as an ideal grid, an output-voltage feedback-controlled converter, and a storage battery, have dominated as input sources for a long time. As a consequence, the scholars and engineers have learned every detail and developed a multitude of power stages and control methods for the voltage domain. A common characteristic of these sources is that their output impedance is low in magnitude at low frequencies. From time to time, a term current-sourced converter has been used with a voltage-sourced converter in case there is an inductor connected in series with the voltage-type source. Unfortunately, such a converter has no explicit relation to the current source as an input source. However, duality implies that there also exist sources that can be classified as real current sources, that is, sources that have an output impedance, which is high in magnitude.

Since the last decade, people have started paying more and more attention on renewable energy sources for providing pollution-free energy and ensuring energy availability also in the future. Usually, most of the power electronic converters applied in interfacing the renewable energy sources into power grid in grid-feeding mode are to be considered as current-fed converters due to the feedback control of DC voltage. Despite the real nature of the input source, the scholars and engineers still like to consider them as voltage sources and justify their opinions by means of Norton–Thevenin transformation. The dual nature of the photovoltaic generators (i.e., current and voltage at specific operation points of their current–voltage curve) makes them an input source that may be too confusing for an engineer to analyze and thus the analysis will be performed in the familiar voltage domain even though such a power source will significantly affect the dynamic behavior of the converters connected at their output terminals. The long history of voltage sources as the dominating input source has created a situation, which has prevented the full understanding of the special features introduced by the current sources as input sources. This is quite understandable, because the most difficult learning process is to learn out from the past.

This book contains material from both of the domains by using the same power stage powered either by the rigid voltage or the current source. The differences in the dynamic behavior of the converters in different domains are explicitly shown including also comprehensive analyses of the source and load interactions in DC–DC converter as well as in grid-connected three-phase converters. Similar material cannot be found from any available book and the material in scientific

papers is scarce and may be hard to identify from the vast number of published papers.

Many individuals have helped us to create the book during the past 20 years in academy. Most of those individuals are our past Ph.D. students and colleagues at TUT, who have created new knowledge during the research projects we have conducted together. We appreciate very much the Finnish industry and funding organizations, who have helped us to fund the research.

Tampere University of Technology
Tampere, Finland

Teuvo Suntio

Tampere University of Technology
Tampere, Finland

Tuomas Messo

ABB Oy
Helsinki, Finland

Joonas Puukko

About the Authors



Teuvo Suntio received his Ph.D. degree in electrical engineering in 1992 from Helsinki University of Technology, Finland. After several R&D engineering and managerial positions during the 22 years in Power Electronics Industry, he accepted a post as a Professor in 1998 in the Electronics Laboratory at University of Oulu, Finland, before moving to Department of Electrical Engineering, Tampere University of Technology in 2004, which is the post he still holds. Professor Suntio's current research interests include dynamic characterization and control of power electronic converters and systems, especially in renewable energy applications. He holds several international patents and has authored or coauthored over 230 international journal and conference publications. He is a Senior Member of IEEE, and has served as an associate editor in *IEEE Transactions on Power Electronics* since 2010.



Tuomas Messo was born in 1985 in Hämeenlinna, Finland. He finalized his M.Sc. and Ph.D. degrees in electrical engineering at Tampere University of Technology (TUT), Tampere, Finland in 2011 and 2014, respectively.

In 2014–2015, he worked as Post-Doctoral Researcher at TUT and in 2016 he was appointed as an Assistant Professor (Tenure Track) in the field of power electronics. He is currently working at the Laboratory of Electrical Energy Engineering at TUT where he carries out lecturing, research, and supervision of electrical engineering students of all degrees.

His main research interests include dynamic modeling of power converters in renewable energy applications and smart grids, impedance-based stability analysis, frequency-domain measurements, control design, and stability analysis of control systems.



Joonas Puukko was born in Helsinki, Finland. He has M.Sc. and Ph.D. degrees (both with distinction) in electrical engineering from the Tampere University of Technology, Tampere, Finland.

He was previously working at ABB Solar Inverters in Helsinki, Finland and ABB Corporate Research Raleigh, NC, USA. At the moment, he is with ABB High Power Drives in Helsinki, Finland. His research interests include power electronics in a range of applications from drives to interfacing of renewable energy systems with the utility grid. He has design experience in wide-bandgap semiconductors, high-frequency magnetics, and frequency-domain modeling/verification.

Part One

Introduction

1

Introduction

1.1 Introduction

For a long time, voltage-type sources such as storage battery, AC grid, and output-voltage-regulated converters have dominated as an input source for power electronic converters [1,2]. These sources are usually referred to as rigid sources, since the load has limited influence on their operating voltage. Both awareness on the depletion of fossil fuel reserves and their impact on the observed climate changes have accelerated the utilization of renewable energy sources, for example, wind and solar [3]. Effective large-scale utilization of these energy sources requires the use of grid-interfaced power electronic converters [4,5]. It has been recently concluded [6,7] that the power electronic converters used in the photovoltaic (PV) systems are essentially current-sourced converters because of the current-source properties of PV generator [8,9] forced by the input-side voltage feedback control [10,11]. At open loop, the static and dynamic properties of the integrating converter are determined by the operating region of the PV generator. The same also applies for the converters in wind energy systems. Another example of a perfect current source is superconducting magnetic energy storage (SMES) system, where a very large inductor serves as the energy storage element [12,13]. Even though the properties of the mentioned sources are already well known [14,15], they are still typically considered as voltage sources when designing the interfacing converter power stages [16,17] or analyzing their underlying dynamics [18–21] despite their current-type properties. The analysis method is usually justified by Norton/Thevenin transformation [20].

The existence of two different input source types implies that two different families of power electronic converters shall also exist, where the converters shall be referred to as voltage-fed (VF) (Figure 1.1) and current-fed (CF) (Figure 1.2) converters, possessing different steady-state and dynamic properties even though the power stage can be the same in both of the cases [7,22]. The term current source has already been widely used, for example, in Ref. [23–28], denoting a voltage-fed converter, where an inductor is placed on the input-side current path such as a boost-type converter [29] or two-inductor (super)buck converter [30]. Fuel cells as renewable energy sources [31] are such an input source, which can be considered to be either voltage or current sources due to their rather constant

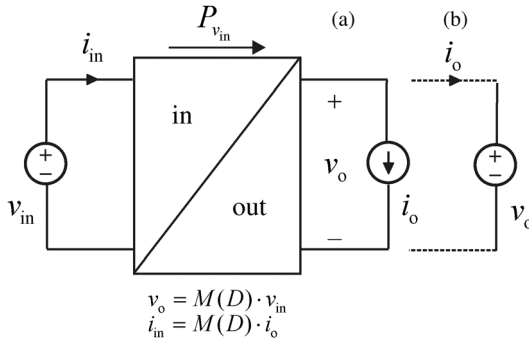


Figure 1.1 VF converter. (a) VO mode. (b) CO mode. *Source:* Suntio 2014. Reproduced with permission of IEEE.

output impedance [32] and operation at the voltages less than the maximum power point [33]. Therefore, the elimination of the harmful low-frequency ripple can be performed by using either input current (i.e., voltage source) or input voltage (i.e., current source) feedback control [34].

On the load side, the output voltage of a converter shall not be taken automatically as an output variable, since this is true only when the converter serves as a typical power supply, regulating its output voltage. In case, the converter is used, for example, as a battery charger or grid-connected inverter, the output voltage is determined by the load-side source and hence output current shall be treated as an output variable. Therefore, the static input-to-output ratio $M(D)$, where D denotes the steady-state duty cycle, shall be actually determined as the ratio of the input-terminal variable characterizing the input source and the same variable at the output terminal, that is, the voltage ratio in a VF converter and the current ratio in a CF converter. According to Figures 1.1 and 1.2, the converter may serve either as a VF or as a CF converter with voltage (VO) or current (CO) as its main output variable, depending on the application. In all the cases, the terminal constraints in terms of voltage and current levels remain unchanged. Reference [22] shows explicitly in theory and by experimental measurements that the dynamic behavior changes significantly application by application as demonstrated in Figure 1.3, where the measured frequency responses of the control-to-output transfer functions with different terminal source configurations are shown. Therefore, it is very important to identify the correct nature of the terminal sources when analyzing the dynamics of the

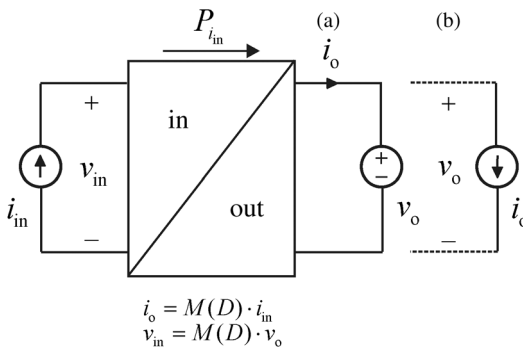


Figure 1.2 CF converter. (a) CO mode. (b) VO mode. *Source:* Suntio 2014. Reproduced with permission of IEEE.

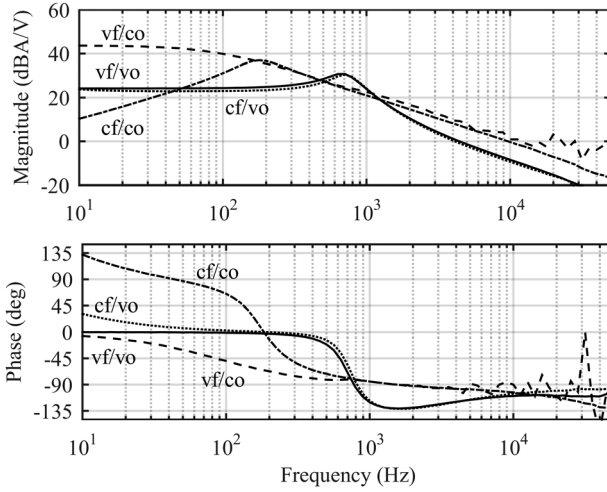


Figure 1.3 The frequency responses of a buck power stage converter when the terminal sources are varied (i.e., voltage-fed converters at voltage (vf/vo) and current (vf/co) output modes and current-fed converters at current (cf/co) and voltage (cf/vo) modes).

converter, for example, for control design purposes, which is obvious when studying the frequency responses in Figure 1.3.

Every power electronic converter has unique internal dynamics, which will determine the obtainable transient dynamics and robustness of stability as well as its sensitivity to the external source and load impedances [35–37]. The internal dynamics can be represented by a certain set or sets of transfer functions, which are classified in circuit theory according to the network parameters [38] known as G (Figure 1.1a), Y (Figure 1.1b), H (Figure 1.2a), and Z (Figure 1.2b), respectively. The specific transfer functions can be directly modeled and measured as frequency responses only when the used terminal sources correspond to the ideal terminal sources given for each of the sets in Figures 1.1 and 1.2. Even if the concept of internal dynamics is basically well known (i.e., all effects from the source and load impedances are removed) [7,35], the tendency is still to use a resistor as a load [39] yielding load-affected models or measured frequency responses. A power stage fed by a certain input source under direct duty ratio (DDR) control tends to maintain the output mode the same as the input source (i.e., VF converters are inherently voltage sources at their output, and CF converters are current sources at their output). As a consequence, the internal transfer functions of such converters can be measured directly at open loop. The other possible output mode does not work at open loop due to violation of Kirchhoff's voltage or current law. The same also applies for the current-mode control, which changes the converter to be a current-output converter [40]. In such a case, the use of resistive load is well justified, but the internal transfer functions have to be computed from the load-affected transfer functions for being useful [7].

A large number of excellent power electronics textbooks are available, such as Refs [5,7,25,39,41–47], which are dedicated to the converters providing either

DC–DC or DC–AC (AC–DC) conversion, or even both. None of these textbooks presents topics that treat the CF converters even if they exist or may even dominate within the specific application area covered in the specific books. The inclusion of the effect of source and load impedances on the converter dynamics is also usually left out by the topics covered in the books even if they are considered very important in practical applications.

The main goal of this book is to provide the missing information in order to complement the other textbooks as well as to present the base for the dynamic analysis of the converters in a general form, which can be utilized with both analytically derived transfer functions and the experimentally measured transfer functions. As a consequence, the potentials of the theoretical work are extended into practice and for the usage of practicing engineers.

The topics covered in the book are briefly discussed and clarified in the subsequent sections in order to familiarize the reader with the secrets of dynamic modeling, analysis, and control designs in both DC-voltage/current source and AC-voltage/current source domains. The mastering of these items requires quite consistent thinking ability as well as flexibility to change from one set of dynamic descriptions to another while moving on.

1.2 Implementation of Current-Fed Converters

There are actually three different methods to implement CF converters: (i) applying capacitive switching cells to construct CF converters [48] similarly as the inductive switching cells are applied, for example, in Refs [1,2], (ii) applying duality transformation methods [49–53], and (iii) adding a capacitor to the input terminal of a VF converter [54] to satisfy the terminal constraints imposed by the input current source [55]. The duality transformation yields CF converters, which retain the main static and dynamic properties characterizing the original VF converter [52]. The adding of a capacitor at the input terminal of a VF converter yields a CF converter having static and dynamic properties resembling the dual of the original converter, that is, a VF buck converter will have characteristics resembling a boost converter and vice versa [54].

As an example, the power stage of a VF buck converter and its dual, that is, the corresponding power stage of a CF buck converter, are given in Figures 1.4 and 1.5. In the original buck converter, the high-side switch S_{HS} conducts during the

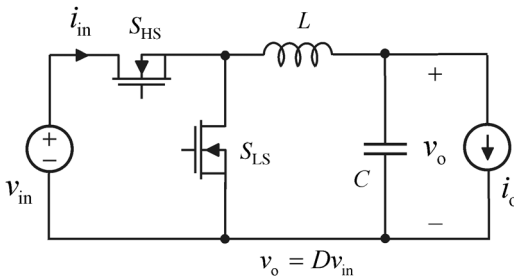


Figure 1.4 VF buck converter.

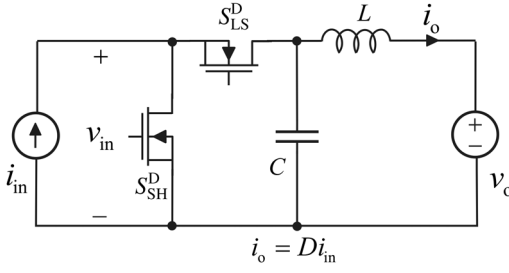


Figure 1.5 CF buck converter.

on-time and the low-side switch S_{LS} during the off-time. In the CF buck converter, the low-side switch S_{LS}^D conducts during the on-time and the high-side switch S_{HS}^D during the off-time. As both of the converters are buck-type converters, the ideal input-to-output relation or modulo $M(D) = D$.

It has been observed earlier that the VF-converter power stages used in the interfacing of PV generators exhibit peculiar properties, such as appearing of right-half-plane (RHP) zero in the control dynamics of buck power stage converter [56], unstable operation when the output voltage or current is tightly controlled [57], necessity to reduce the pulsewidth for increasing the output variables [58,59], and appearing of RHP pole when peak-current-mode (PCM) control is applied in a buck power-stage converter [60,61], and even the impedance-based stability assessment has to be performed differently compared to the VF converters [62]. The observed phenomena are good evidence for the necessity to fully take into account the used terminal sources as discussed in Ref. [22].

1.3 Dynamic Modeling of Power Electronic Converters

The methods to develop the required small-signal or dynamic models for the power electronic converters date back to the early 1970s [63] when the foundation for the state space averaging (SSA) method was laid down [64] and later modified to correctly capture the dynamics associated with the discontinuous conduction mode (DCM) of operation [65,66] as well as with the variable frequency operation [67,68]. The same methods also apply equally to modeling the dynamics of three-phase grid-connected power converters [69]. The SSA method is observed to produce accurate models up to half the switching frequency.

One of the most fundamental issues in performing the modeling in addition to the recognition of the correct input and output variables is that the state variables are to be considered as the time-varying average values within one switching cycle of the corresponding instantaneous values [66]. In continuous conduction mode (CCM), this is also true in the instantaneous state variables and, therefore, the averaged state space can be constructed by computing the required items directly by applying circuit theory. The continuity is also reflected as the known length of the on-time and off-time. In DCM, the instantaneous variables are not anymore necessarily continuous signals but rather pulsating signals, which is also reflected as the unknown length of off-time. Therefore, their time-varying average values

have to be computed based on the wave shapes of their instantaneous values and used for computing the length of the unknown off-time. A number of variants are available for the basic SSA method in continuous time as well as in discrete time, which can also be used for obtaining the dynamic models but they do not offer usually such benefits, which would justify their usage in practical applications.

The original SSA method can be applied as such only to the converters, which operate in CCM under DDR control, which is also known as voltage-mode (VM) control [39]. The last term is not recommended, however, to be used, because it will mean in the future the internal control methods in a CF converter, where the feedback is taken from the capacitor voltage (i.e., peak voltage mode (PVM) or average voltage mode (AVM)) similarly as the current-mode controls (i.e., peak current (PCM) or average current (ACM)) in a VF converter. The dynamic models (i.e., the small-signal state space) induced by the DDR control will serve as the base for the modeling of the converters, where the internal feedback loops are used to affect the duty ratio generation, that is, the dynamics associated with the duty ratio. The modeling of those converters can be simply done by developing proper duty-ratio constraints, where the perturbed duty ratio is expressed as a function of the state and input variables of the converter [7]. In case of variable-frequency operation, the duty ratio is nonlinear and, therefore, the on-time of the switches has to be used as the control variable instead of duty ratio [7,68].

1.4 Linear Equivalent Circuits

As an outcome of the SSA modeling method [64], the dynamics of the associated converter was represented by means of the canonical equivalent circuit given in Figure 1.6, which is valid for a second-order or two-memory-element converter operating in CCM under DDR control. The structure and the circuit elements of the equivalent circuit can be found from the corresponding small-signal state space. Similar equivalent circuit can also be constructed for the higher order converters as well as for CF converters (see Figure 1.7) applying the same methodology. Figures 1.6 and 1.7 provide clear physical insight into the dynamic processes inside the converters as well as clearly indicate the differences the

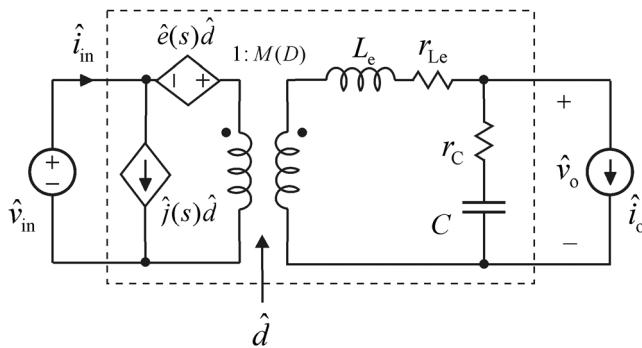


Figure 1.6 Canonical equivalent circuit for a second-order VF/VO converter.

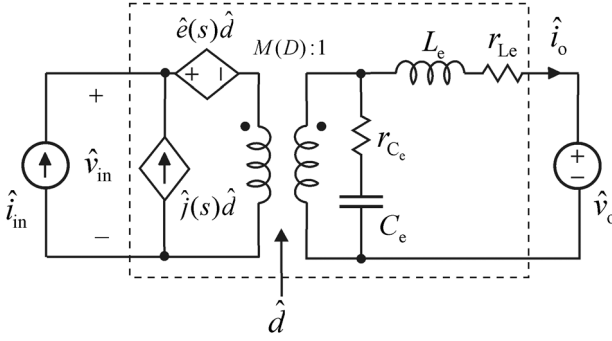


Figure 1.7 Canonical equivalent circuit for a second-order CF/CO converter.

duality transformation produces in the converter. As being a linear representation of the converter, the effect of the source and load impedances can be computed by applying circuit theory, which is very important for understanding the dynamic behavior of the practical systems.

Similar equivalent circuits as in Figures 1.6 and 1.7 cannot be, however, constructed for the converters operating in DCM or containing internal feedbacks, for example, PCM control. More general equivalent circuit can be constructed based on the set of transfer functions comprising the network parameters G , Y , H , and Z , which can be utilized similarly as the canonical equivalent circuits in Figures 1.6 and 1.7 to assess the effect of nonideal source and load [7,70]. Figures 1.8 and 1.9 show such a generic equivalent circuit representing the dynamics of VF/VO DC–DC and a VF/CO DC–DC converters, respectively. On comparing the equivalent circuits in Figures 1.6 and 1.7 with the equivalent circuits in Figures 1.8 and 1.9, the main difference found between them is that the latter equivalent circuits present explicitly the main terminal characteristics of a converter. This information is actually very important for being able to fulfill the terminal constraints stipulated by the different input and output sources.

Similar equivalent circuits as in Figures 1.6 and 1.7 can also be constructed for the three-phase grid-connected converters by means of their small-signal state space given in the synchronous reference frame applying power invariant transformation (i.e., power-invariant d–q state space), as shown in Figures 1.10 and 1.11 [71,72]. The corresponding physical schematics are given in Figures 1.12

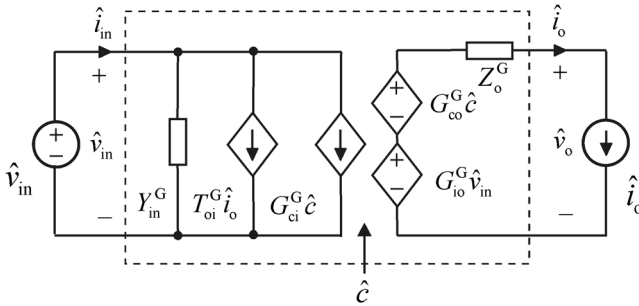


Figure 1.8 Generic equivalent circuit for a VF/VO converter.

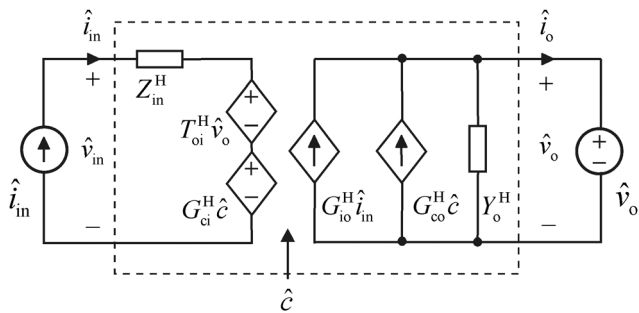


Figure 1.9 Generic equivalent circuit for a CF/CO converter.

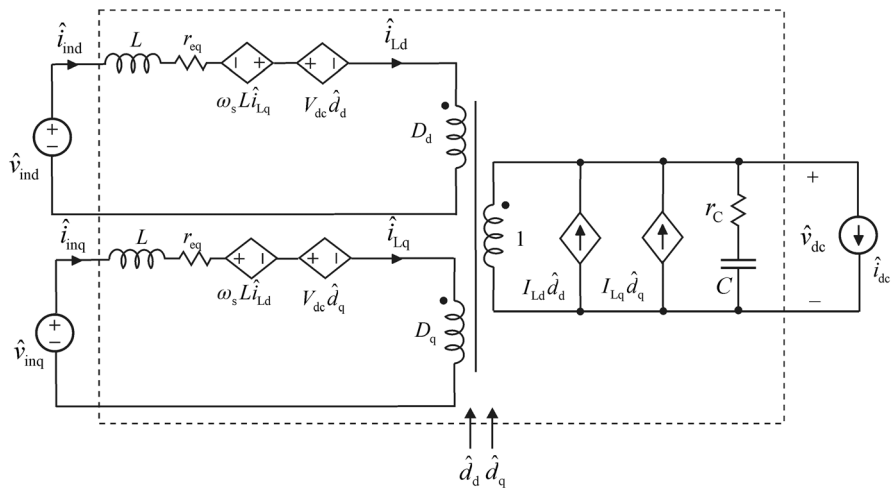


Figure 1.10 Canonical equivalent circuit for a three-phase AC-DC converter.

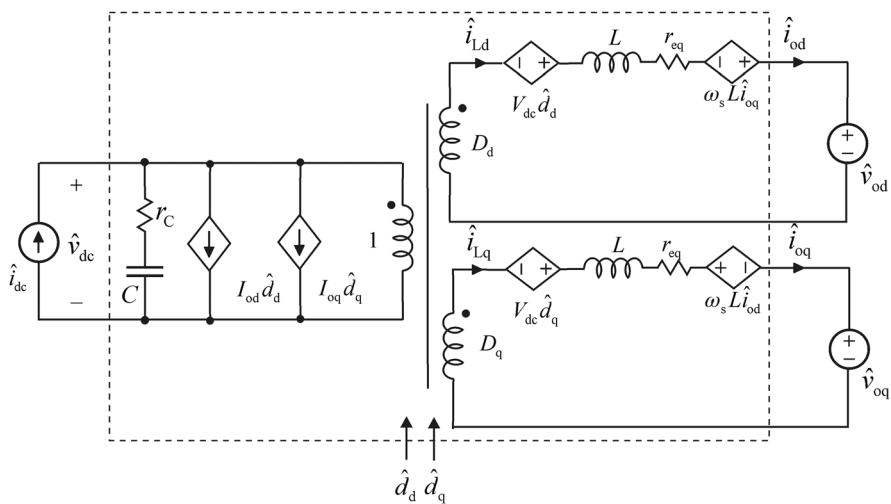


Figure 1.11 Canonical equivalent circuit for a current-fed three-phase DC-AC converter.

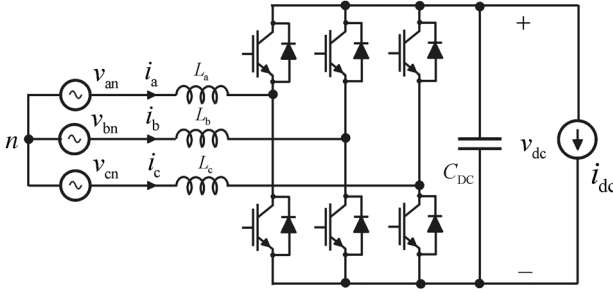


Figure 1.12 Three-phase grid-connected rectifier.

and 1.13, respectively. According to Figures 1.12 and 1.13, the converters can be constructed from each other by changing the direction of power flow. This similarity is also visible in the corresponding equivalent circuits. These equivalent circuits would give the same physical insight as the corresponding DC–DC equivalent circuits.

Similar equivalent circuits as in Figures 1.10 and 1.11 cannot be, however, constructed for the converters operating in DCM or containing internal feedbacks. Similarly, as in the case of DC–DC converters, the more general equivalent circuits can be constructed based on the set of transfer functions comprising the network parameters G , Y , H , and Z , which can be utilized similarly as the canonical equivalent circuits in Figures 1.10 and 1.11 to assess the effect of nonideal source and load [7,73]. Figure 1.14 shows such a generic equivalent circuit representing the dynamics of a three-phase grid-connected AC–DC converter, and Figure 1.15 shows a generic equivalent circuit representing the dynamics of a three-phase grid-connected current-fed inverter. On comparing the equivalent circuits in Figures 1.10 and 1.11 with the equivalent circuits in Figures 1.14 and 1.15, the main difference found between them is that the latter equivalent circuits present explicitly the main terminal characteristics of a converter. This information is actually very important for being able to fulfill the terminal constraints stipulated by the different input and output sources.

The variables of the equivalent circuits with a superscript s denote the three-phase variables transformed into the synchronous reference frame (SRF) composed of direct (d) and quadrature (q) components of the variables, respectively. The

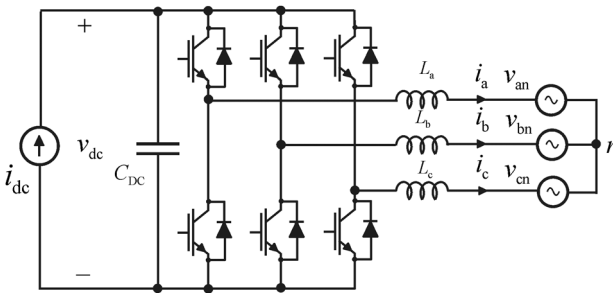


Figure 1.13 Three-phase grid-connected current-fed inverter.

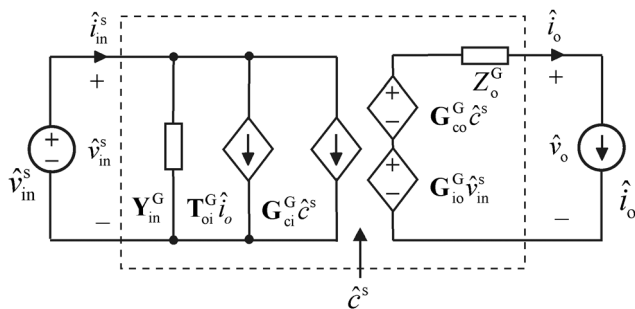


Figure 1.14 Generic equivalent circuit for a three-phase grid-connected VF/VO converter.

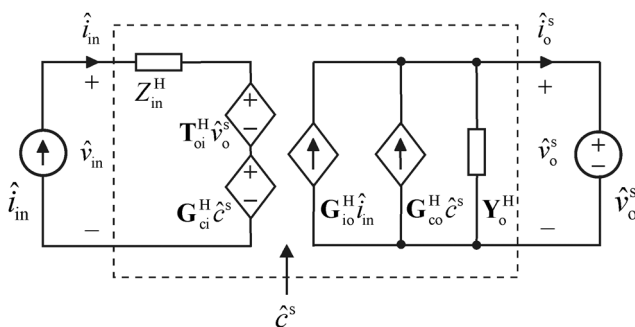


Figure 1.15 Generic equivalent circuit for a three-phase grid-connected CF/CO converter.

transfer functions represented with boldface letters denote a transfer function matrix composed of two or four discrete transfer functions. The computation of the effect of nonideal source and load has to be performed by applying matrix manipulation techniques instead of circuit theoretical methods [73].

The generic equivalent circuits are very flexible tools for solving the dynamic problems associated with the impedance-based interactions [37,71,74] as well as for assessing the stability in the practical interconnected systems [75,76]. The dynamic equivalent circuits as well as the corresponding matrix-form representations can be equally utilized by means of the model-based analytic transfer functions and the corresponding measured frequency responses or even by their combination.

1.5 Impedance-Based Stability Assessment

Stability assessment of a system composed of interconnected power electronic converters as well as passive impedance-like elements can be effectively performed at any interface within the system by means of the ratio of upstream and downstream impedances measured or predicted at the interface [7,22,63,75–84].